International Journal of Nanoelectronics and Materials
IJNeaM
ISSN 1985-5761 | E-ISSN 2232-1535

Investigation of Material and Structural Effects on MEMS Thermal Sensor Characteristic

Mohd Hafiz Ismail[a,*], Bibi Nadia Taib[a], Shazlina Johari[b], Hasnizah Aris[c] and Linda Silvia[d]

[a]*Faculty of Electronic Engineering & Technology, Universiti Malaysia Perlis, Kampus Alam UniMAP, Pauh Putra, 02600 Arau, Perlis, Malaysia*
[b]*Institute of Nano Electronic Engineering, Universiti Malaysia Perlis*
[c]*Centre of Excellence for Micro System Technology (MiCTEC), Universiti Malaysia Perlis, Arau, 02600, Perlis, Malaysia*
[d]*Institut Teknologi Sepuluh Nopember, Surabaya, Indonesia*
**Corresponding author. Tel.: +60-04988-5549; e-mail: shazlinajohari@unimap.edu.my*

Received 24 Sept 2025, Revised 25 Nov 2025, Accepted 21 May 2026

ABSTRACT

In this paper, the design, simulation, and analysis of a MEMS-based thermal sensor are presented using MEMSPro and ANSYS. The study aims to assess the effect of significant design parameters on the sensor's performance. The sensor was *virtually fabricated in MEMSPro using standard microfabrication processes*, *including* photolithography, deposition, and etching. ANSYS software was used to conduct finite element analysis in order to observe the sensor's thermal response under varying conditions. Four primary parameters were *investigated: coil materials (brass, gold, and copper), coil thicknesses (1 µm, 3 µm, and 6 µm), parylene types (Parylene-C, -F, and -N), and input temperatures* ranging from 10 °C to 90 °C. The results demonstrate that these parameters significantly influence the average temperature and electrical resistance across the sensor. Brass exhibited the highest average temperature, while Parylene-N, with the highest thermal conductivity, produced the greatest thermal response. These findings provide insights into optimizing MEMS thermal sensor designs for enhanced sensitivity and stability, with potential applicability in real-time temperature monitoring systems.

Keywords: *MEMS, thermal sensors, MEMSPro, ANSYS, Parylene*

1. INTRODUCTION

Micro-Electro-Mechanical Systems (MEMS) thermal sensors have attracted significant research interest due to their ability to detect temperature variations at the microscale with high sensitivity and the potential for compact integration [1-4]. MEMS based thermal sensors are widely utilized in industrial process monitoring, biomedical technique of diagnosis, and environmental sensing, where accurate temperature measurement and stability are required. The performance of MEMS thermal sensors typically depends on its material properties such as thermal conductivity and coefficient of thermal expansion, as well as structural parameters of the sensors which include coil geometry, membrane material, and thickness.

Previous work on improving MEMS thermal sensor performance has been reported. For example, Lee et al. [5] have demonstrated the fabrication of micro temperature sensors on flexible substrates. This highlights the importance of substrate compatibility in expanding the application of MEMS thermal sensors. Kedia and Wang [6] investigated MEMS-based resettable circuit breakers, emphasizing the role of thermal sensing elements in protective electronics. Li et al. [7] analysed electromagnetic-thermal-electric interactions in RF MEMS power sensors, showing that thermal response depends highly on the resistor geometry. Similarly, Dalola et al. [8] and Yi et al. [9] reported on MEMS thermal flow and microwave power sensors, respectively, showing that material selection and structural design critically determine sensitivity, resistance variation, and long-term stability.

Despite these reported advances in the field, several research gaps remain. Most prior studies focused on either sensor design or fabrication processes, with limited focus on correlating sensors' material choices, such as coil composition, structural parameters, such as thickness, and dielectric membrane properties, such as parylene type, with overall thermal response and resistance characteristics. Furthermore, while many investigations focus on single-parameter optimization, there is still a lack of comprehensive comparative analysis that evaluates multiple parameters simultaneously under controlled conditions. This leaves uncertainty in determining optimal design approaches to achieve a good trade-off among sensitivity, thermal stability, and fabrication feasibility.

To address these gaps, this study presents a design, simulation, and analysis of a MEMS thermal sensor using MEMSPro and ANSYS software. By varying coil material of brass, gold, copper, coil thickness of 1 µm, 3 µm, 6 µm, parylene membrane type of Parylene-C, -F, -N, and input temperature range from 10 °C to 90 °C, this work investigates their influence on average temperature distribution and electrical resistance. The findings aim to provide design guidelines for optimizing MEMS thermal sensors toward enhanced sensitivity, robustness, and application versatility. This paper investigates the effects of varying key parameters on the operating principle of a

MEMS thermal sensor. It outlines the fabrication process for the sensor and describes the initial design parameters. Four main parameters are varied to analyze their impact on the sensor's performance: the type of coil material, coil thickness, type of parylene membrane, and the applied input temperature. The results of this analysis focus on how each parameter influences the average temperature measured by the thermal sensor.

2. MEMS THERMAL SENSOR DESIGN

2.1. Operating Principle

The MEMS thermal sensor, as illustrated in Figure 1, operates based on the principle of temperature-induced resistance variation. When different temperatures are applied at both ends of the coil, a thermal gradient is established along its length. This results in a measurable average temperature across the coil. An external circuit or device, based on resistance, such as a voltage divider in the instrument, is connected to the average temperature and can then differentiate the resistance based on the temperature.

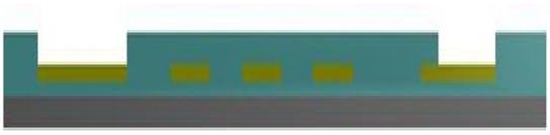

Figure 1. Cross-section view of the MEMS thermal sensor.

2.2. Equations

Resistance is calculated by applying different temperatures at both ends of the coil, as shown in Equations (1) to (3). The resistance of a typical metal can be represented by the formula where R denotes the resistance (in ohms), ρ is the resistivity (in ohmmeters), L is the length of the wire (in meters), and A is the cross-sectional area (in square meters) in Equation 1. When the temperature of the Resistance Temperature Detector (RTD) changes linearly, the correlation between the measured resistance and the temperature shift, where R_t denotes the resistance at t °C, R_i represents the resistance at I °C, and α_T is indicative of the sensitivity, is given in Equation 2. In Equation 3, the sensitivity of the MEMS thermal sensor, α_T is calculated based on the rearrangement of Equation 2.

$$R = \rho L/A \quad (1)$$

$$R_t = R_i(1 + \alpha_T \Delta T) \quad (2)$$

$$\alpha_T = (R_t - R_i)/R_i(\Delta T) \quad (3)$$

2.3. Design Dimensions and Specification

The designs of the MEMS thermal sensor are created in ANSYS with four different types of parameters, as depicted in Figure 2, with the device parameters listed in Table 1. The design parameters include the types of coil material, the thickness of the coil, the types of Parylene, and the input temperature.

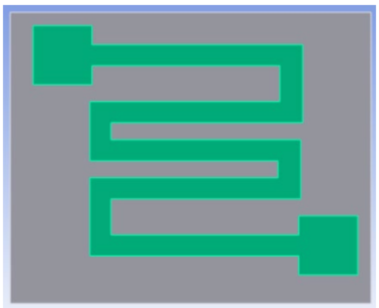

(a)

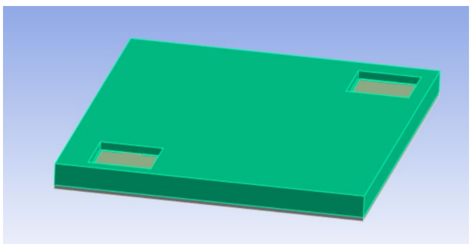

(b)

Figure 2. MEMS thermal sensor with (a) types of coil material and (b) the thickness of the coil.

Table 1 Device Parameters

Parameter Types	Device Parameters
Coil Materials	Brass
	Gold
	Diamond
Coil Thickness	1 μm
	3 μm
	6 μm
Parylene Types	Parylene-C
	Parylene-N
	Parylene-F
Input Temperature (°C)	10
	30
	50
	70
	90

3. RESULTS AND DISCUSSIONS

The MEMS Thermal Sensor undergoes fabrication simulation using MEMSPro, and finite element analysis is conducted using ANSYS.

3.1. MEMSPro Fabrication Simulation

The fabrication simulation of the MEMS Thermal Sensor is carried out using MEMSPro, following the process steps outlined in Table 2. The designed layout includes substrate, coil and Parylene. The ultimate layout of the MEMS Thermal Sensor is depicted in Figure 3.

Table 2 Fabriation Process Steps

Step No.	Step Name	Command	Material	Thickness (μm)
1	Wafer	Wafer	Silicon	2
2	Deposit Parylene	Deposit	Parylene	1
3	Deposit Photoresist	Deposit	Photoresist	1
4	Photolithography	Etch	Photoresist	1
5	Deposit Gold	Deposit	Gold	1
6	Etch Gold	Etch	Gold	1
7	Etch Photoresist	Etch	Photoresist	1
8	Deposit Parylene	Deposit	Parylene	2
9	Deposit Photoresist	Deposit	Photoresist	1
10	Etch Anchor	Etch	Photoresist	3
11	Etch Photoresist	Etch	Photoresist	-

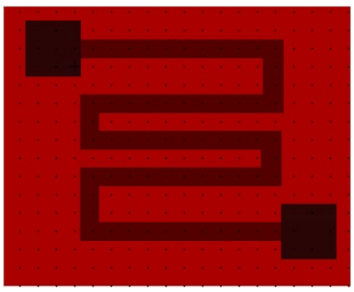

Figure 3. Final Layout of MEMS thermal sensor in MEMSPro Layout Editor.

Figure 4 illustrates the simulation of the MEMS thermal sensor fabrication process using MEMSPro. Meanwhile, Figure 5 shows the final 3D model of the MEMS thermal sensor upon completion of all fabrication steps.

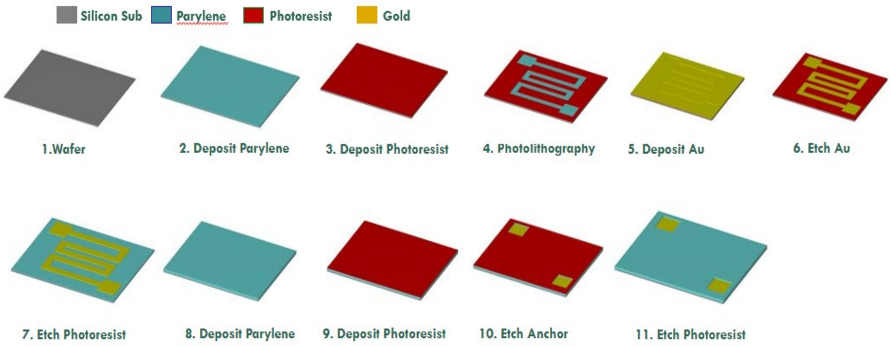

Figure 4. MEMS thermal sensor fabrication process simulation in MEMSPro.

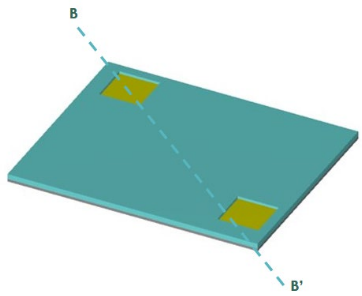

Figure 5. 3D model of MEMS thermal sensor.

3.2. ANSYS Finite Element Analysis

Upon finishing the seven steps of finite element analysis in ANSYS, the results reveal the average temperature of the MEMS Thermal Sensor under different input temperatures applied at both ends of the coils, as illustrated in Figure 6 and Figure 7.

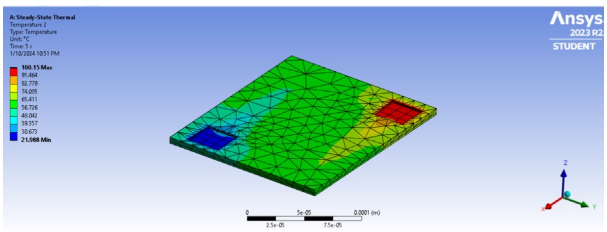

Figure 6. Thermal simulation of MEMS thermal sensor.

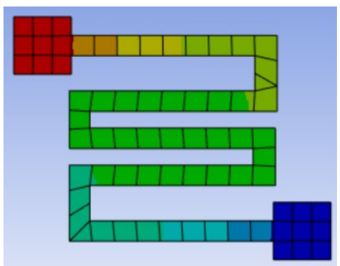

Figure 7. Temperature distribution along a Coil.

Table 3 and Figure 8 are the result of changing materials of the coil of MEMS thermal sensor in ANSYS.

Table 3 Average Temperature With Variation of Materials of the Coil

Coil Materials	Average Temperature (°C)	Average Temperature on Probe (°C)
Brass	61.026	60.118
Gold	61.024	58.489
Copper	61.022	58.030

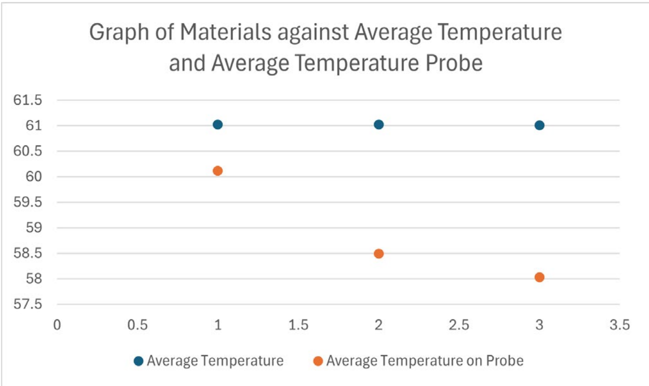

Figure 8. Average temperature with variation of materials of the coil.

The input temperature at one end of the coil is 100 °C, while the other end is maintained at 22 °C. A temperature probe is placed at the center of the coil. After running the simulation, the average temperature was measured and plotted on a graph. Initially, gold was used as the coil material, followed by brass and copper. The average temperatures recorded for gold, brass, and copper were 61.026 °C, 61.024 °C, and 61.022 °C, respectively. Overall, brass exhibited the highest average temperature, while copper showed the lowest. Gold's average temperature was intermediate between the two. As the average temperature increases, the coil's resistance also tends to increase. Table 4 and Figure 8 are the result of the resistance of the different coil materials of MEMS thermal sensor in ANSYS.

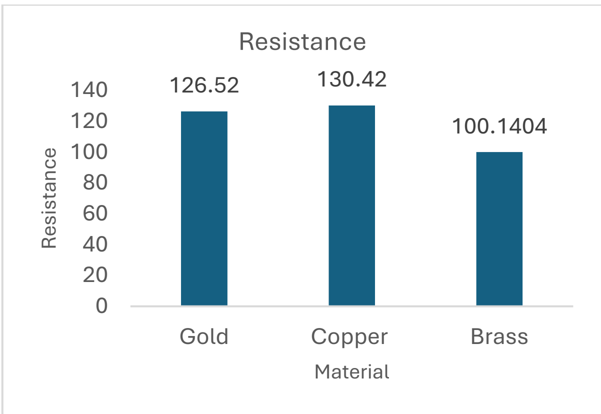

Figure 9. Graph of resistance of the different coil materials.

Table 4 Resistance With Variation of Materials of the Coil

Material	Thermal Coefficient (°C)	Resistance (Ω)
Gold	0.003400	126.5200
Copper	0.003900	130.4200
Brass	0.000018	100.1404

Based on the result, it can be concluded that the resistance of materials increases as the thermal coefficient increases. The maximum and minimum temperatures are the same when changing the materials. Table 5 and Figure 10 show the results of varying the coil thickness in the MEMS thermal sensor simulation conducted using ANSYS.

Table 5 Average Temperature With Variation of Thickness of the Coil

Thickness Parylene (μm)	Thickness Coil (μm)	Average Temperature (˚C)	Average Temperature on Probe (˚C)
3	1	61.057	59.475
5	3	61.04	58.873
8	6	61.021	57.953

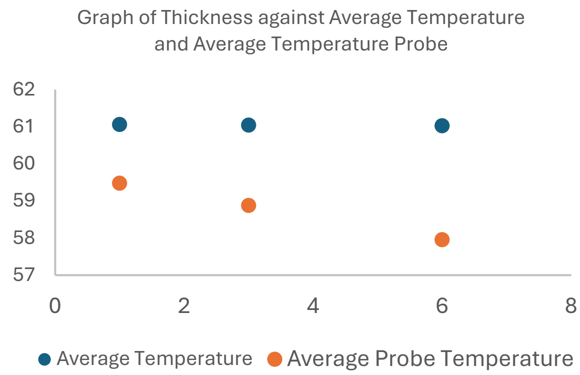

Figure 10. Graph of thickness variation of the coil against temperature.

By comparing the average temperature after the thickness of the coil varies, the average temperature decreases, as the thickness of the coil increases. Parylene here works as an insulator to make sure heat is not dissipated to the surroundings where it may cause heat loss. Therefore, the type of Parylene may slightly affect the average temperature of the MEMS thermal sensor. Different types of Parylene have different thermal conductivity values. Table 6 and Figure 11 show the results of changing the type of Parylene used in the MEMS thermal sensor.

Table 6 Type of Parylene With Thermal Conductivity and Obtain Average Temperature

Type of Parylene	Thermal Conductivity ($Wm^{-1}K^{-1}$)	Average Temperature (˚C)
Parylene-C	0.084	61.057
Parylene-F	0.1	61.06
Parylene-N	0.126	61.064

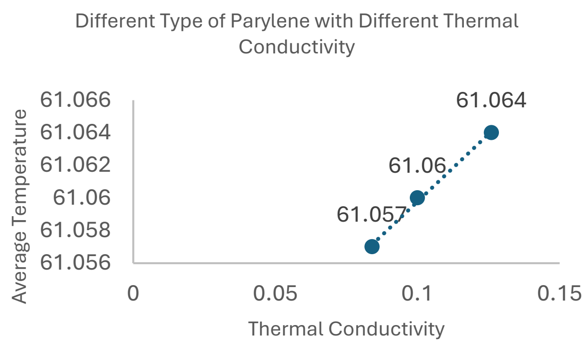

Figure 11. The effect of different types of Parylene on the average temperature in ANSYS.

Based on the results, Table 6 and Figure 11 show that the average temperature increases with thermal conductivity, even when the applied temperature is constant. Parylene-N, which has the highest thermal conductivity, yields the highest average temperature, followed by Parylene-F and Parylene-C.

In this section, the minimum temperature values were varied. The new values are compared with the control temperature of 22°C. From the new values, the average temperature was measured and recorded. Table 7 shows the readings for minimum, maximum, and average temperature.

Table 7 Measurements of The Minimum Temperatures and Their Respective Average Temperatures

Minimum Temperature (°C)	Maximum Temperature (°C)	Average Temperature (Ω)
10	100	55.066
30	100	65.052
50	100	75.037
70	100	85.022
90	100	95.007

Table 8 shows the rough estimation of where the average temperature is measured on the structure using the temperature probe.

Table 7 Measurements of Average Temperatures Using The Temperature Probe

Times (s)	Temperature Probe(°C)
1	53.240
2	63.631
3	74.022
4	84.413
5	94.804

The relationship between temperature and resistance is given by Equation (2). Figure 12 shows a steady increase in resistance as the difference in temperature increases.

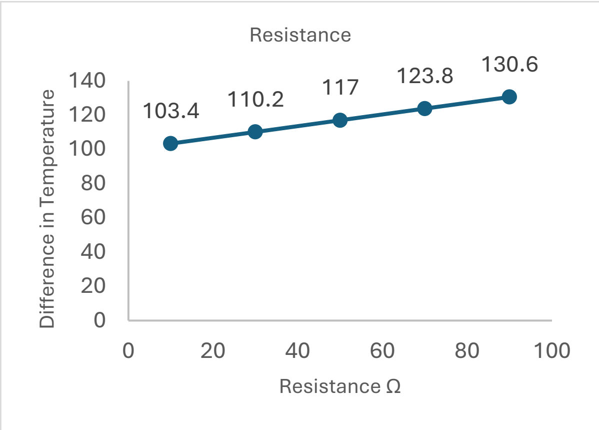

Figure 12. Relationship between difference in temperature and resistance.

Based on the results, it can be concluded that the resistance of materials increases with average temperature.

The simulation results clearly demonstrate that material and structural parameters play a critical role in determining the performance of MEMS thermal sensors. Among the coil materials tested, brass exhibited the highest average temperature, compared to gold and copper, implying greater sensitivity to thermal gradients. However, its resistance value was significantly lower due to its smaller temperature coefficient. This suggests that while brass maximises heat retention, gold and copper may offer greater stability in resistance-based sensing applications. This observation is in agreement with the work reported by Li et al. [7], who focused on the importance of resistor dimensions and materials when investigating the electromagnetic-thermal coupling behavior of MEMS sensors. We also observe the effect of coil thickness: as the thickness increased from 1 μm to 6 μm, the average temperature measured at the probe decreased. This inverse relationship suggests that thinner coils are more effective in maintaining temperature gradients, hence improving the sensor response. Similar observations were made by Kedia and Wang [6], who reported that thinner conductive layers can improve sensitivity, but this could affect the sensor's structural robustness. This trade-off highlights the need for careful optimization of coil dimensions depending on application requirements, in which sensitivity or long-term durability are the main priorities. The role of the Parylene membrane was further investigated by comparing

Parylene-C, -F, and -N. The results showed that Parylene-N, having the highest thermal conductivity, produced the greatest average temperature, followed by Parylene-F and Parylene-C. This suggests that dielectric membrane selection directly affect thermal transfer efficiency and, consequently, sensor response. These findings are consistent with Dalola et al. [8], who reported that sensor encapsulation materials with higher thermal conductivity can significantly enhance output signals in MEMS flow sensors. The variation in input temperature also confirmed the direct relationship between thermal gradients and resistance. As the input of temperature difference increased, the resistance across the coil rose steadily. This trend is consistent with the linear relationship predicted by Equation (2) in the model, reaffirming that MEMS thermal sensors operate reliably under varying temperature ranges. Compared to Yi et al. [9], who demonstrated a similar resistance–temperature correlation in microwave MEMS power sensors, the present study extends these findings by providing a systematic multi-parameter analysis rather than focusing on a single design factor.

Overall, the results validate the hypothesis that multi-parameter optimisation—combining coil material selection, thickness control, and parylene type—is necessary to achieve an optimal balance between sensitivity, stability, and fabrication feasibility. While brass coils and Parylene-N provide the most promising results in terms of thermal response, gold or copper may be preferable for applications requiring consistent resistance behavior. These findings therefore bridge the research gap identified in earlier studies by providing a comparative evaluation of various material and structural combinations and offering practical design guidelines for future MEMS thermal sensor development.

4. CONCLUSIONS

In this paper, a MEMS thermal actuator sensor was designed, simulated and analyzed using ANSYS Academic and MEMSPro software. By using the MEMSPro Software, the 3D model of the MEMS thermal actuator was generated. The process definition, materials and layout were also defined during the initial process. The material properties of the MEMS thermal actuator were specified. To fabricate the individual layers of the structure, the fabrication process was defined for each material. In summary, there were a few key findings found in this project. Changing the type of material in the coil affected the material's resistance to voltage. The thickness of the coil also played a role in the coil's average temperature. Additionally, the average temperature depends on the type of Parylene. Last but not least, the input temperature also affects the voltage resistance of the coil. Through these analyses, we determined the most suitable parameters for this project.

ACKNOWLEDGMENT

Thanks to the Faculty of Electronic Engineering Technology at Universiti Malaysia Perlis, the authors were able to design, simulate, and analyze the MEMS capacitive pressure sensor using ANSYS and MEMSPro software.

REFERENCES

[1] Algamili, A.S.; Khir, M.H.; Ahmed, A.Y.; Rabih, A.A.; Ba-Hashwan, S.S.; Alabsi, S.S.; Al-Mahdi, O.L.; Isyaku, U.B.; Ahmed, M.G.; Junaid, M. Fabrication and Characterization of the Micro-Heater and Temperature Sensor for PolyMUMPs-Based MEMS Gas Sensor. *Micromachines* **2022**, *13*, 525. https://doi.org/10.3390/mi13040525.

[2] W. Xu *et al.*, "A Sub-5mW Monolithic CMOS-MEMS Thermal Flow Sensing SoC With ±6 m/s Linear Range," in *IEEE Journal of Solid-State Circuits*, vol. 59, no. 5, pp. 1486-1496, May 2024, doi: 10.1109/JSSC.2023.3314765.

[3] Lee, H.-J.; Park, D.-J. Analysis of Thermal Characteristics of MEMS Sensors for Measuring the Rolling Period of Maritime Autonomous Surface Ships. *J. Mar. Sci. Eng.* **2022**, *10*, 859. https://doi.org/10.3390/jmse10070859

[4] T. Dinh, H. -P. Phan, A. Qamar, P. Woodfield, N. -T. Nguyen and D. V. Dao, "Thermoresistive Effect for Advanced Thermal Sensors: Fundamentals, Design Considerations, and Applications," in *Journal of Microelectromechanical Systems*, vol. 26, no. 5, pp. 966-986, Oct. 2017, doi: 10.1109/JMEMS.2017.2710354.

[5] C.-Y. Lee, S.-J. Lee, and G.-W. Wu, "Fabrication of Micro Temperature Sensor on the Flexible Substrate," 2007.

[6] S. Kedia and W. Wang, "Simulation, design, fabrication, and testing of a MEMS resettable circuit breaker," Journal of Microelectromechanical Systems, vol. 24, no. 1, pp. 232–240, Feb. 2015, doi: 10.1109/JMEMS.2014.2328996.

[7] J. H. Li, X. Liao, and C. Chu, "Electromagnetic-thermal-electric analysis of indirectly-heated RF MEMS power sensors with different terminal resistor dimensions," IEEE Sens J, vol. 21, no. 4, pp. 4342–4349, Feb. 2021, doi: 10.1109/JSEN.2020.3033011.

[8] S. Dalola et al., "MEMS thermal flow sensor with smart electronic interface circuit," IEEE Sens J, vol. 12, no. 12, pp. 3318–3328, 2012, doi: 10.1109/JSEN.2012.2219619.

[9] Z. Yi, H. Yan, J. Yan, and X. Liao, "Fabrication of the differential microwave power sensor by seesaw-type MEMS membrane," Journal of Microelectromechanical Systems, vol. 25, no. 4, pp. 582–584, Aug. 2016, doi: 10.1109/JMEMS.2016.2569610.